

## Supplementary Information for:

# Core-satellite assembly of gold nanoshells on solid gold nanoparticle for color coding plasmonic nanosensor

*Nguyen H. Le,<sup>a</sup> Nicole Cathcart,<sup>a,b</sup> Vladimir Kitaev<sup>b</sup> and Jennifer I. L. Chen<sup>a\*</sup>*

<sup>a</sup>Department of Chemistry, York University, 4700 Keele Street Toronto, Ontario, M3J 1P3,  
Canada.

<sup>b</sup>Department of Chemistry and Biochemistry, Wilfrid Laurier University, 75 University Ave. W.,  
Waterloo, Ontario N2L 3C5, Canada

Email: [jilchen@yorku.ca](mailto:jilchen@yorku.ca)

## SUPPORTING FIGURES

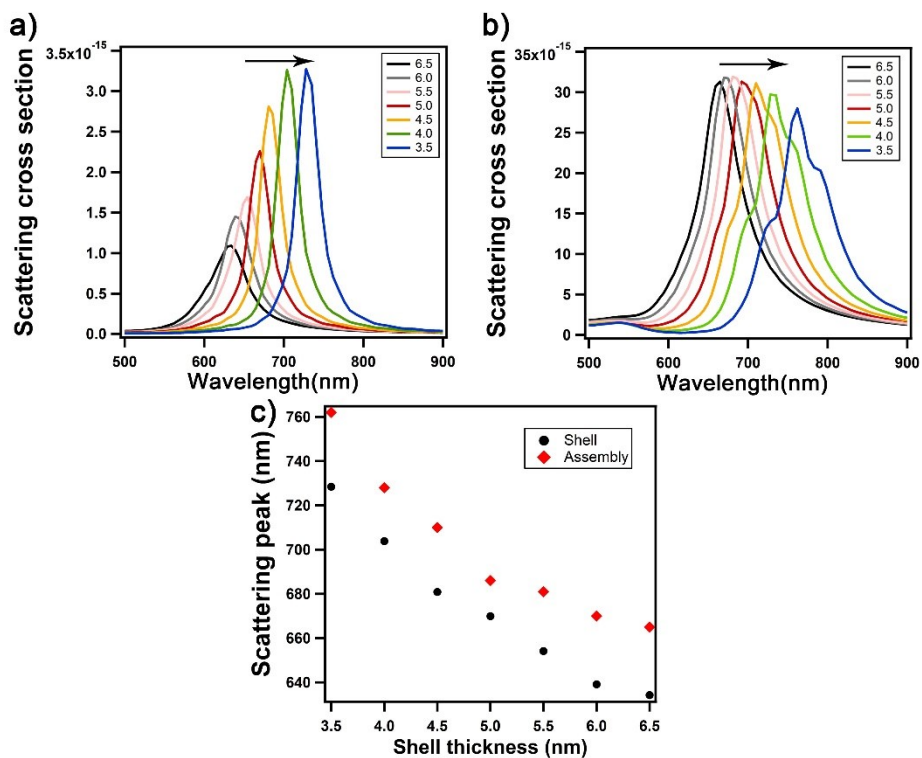


**Figure S1.** FDTD simulated scattering spectra: (a) Single 45-nm Au nanoshell with various thicknesses (3.5 – 6.5 nm), and (b) solid-shell assemblies with 5 satellite particles of the corresponding nanoshells. (c) Comparison of scattering peak wavelengths of nanoshells (black circle) and solid-shell assemblies (red diamond) vs shell thickness.

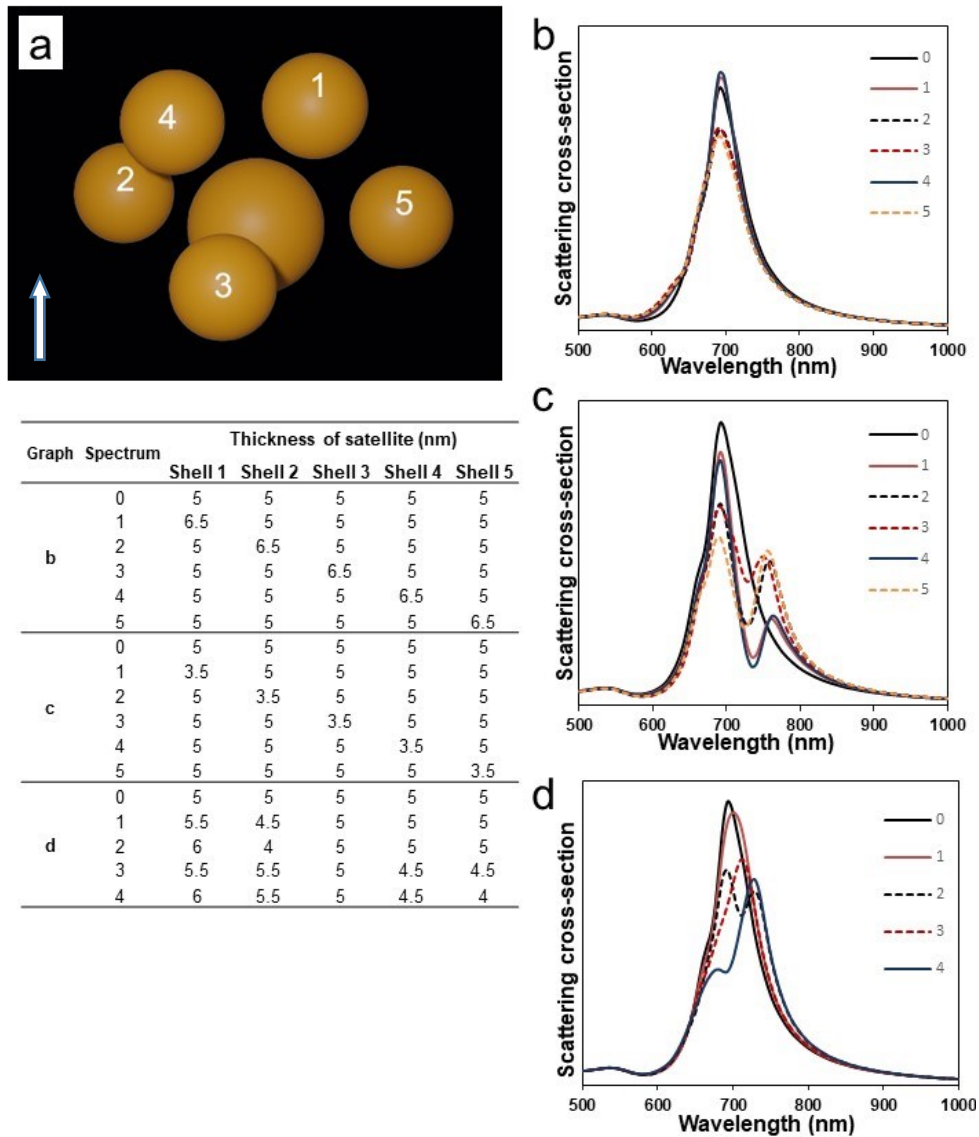


**Figure S2.** Sensitivity of LSPR scattering on thickness variations of satellite nanoshells in an assembly structure. (a) Structure of the 5-nanoshell assembly employed with each shell particle numbered. Simulated unpolarized scattering spectra of assemblies with all nanoshells having 5-nm thickness (black curve in b, c and d), and (b) one satellite thicker (6.5 nm) vs (c) one satellite thinner (3.5 nm). Legend denotes the nanoshell that was varied. (d) Scattering spectra of assemblies having an overall average shell thickness of 5 nm, but with different thicknesses in two or four satellite nanoshells as summarized in the table.

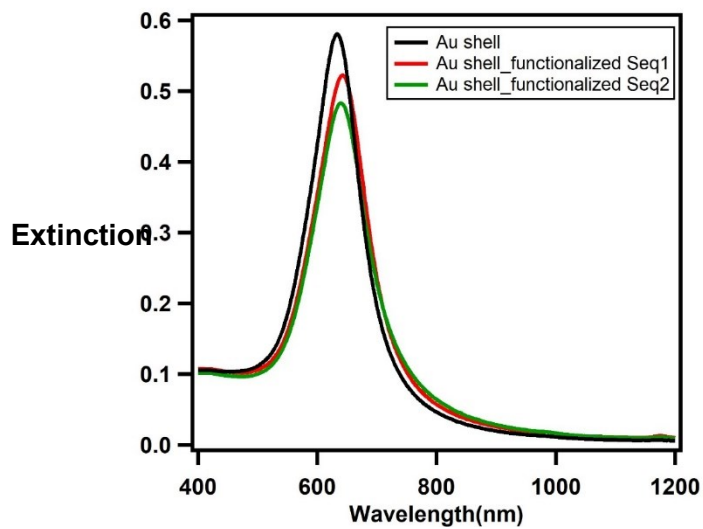


**Figure S3.** Extinction spectra of decahedral Au nanoshells in water (black), and functionalized with Seq 1 (red) and Seq 2 (green). The refractive index (RI) of a dense layer of ssDNA on Au was reported to be 1.46.<sup>1</sup> In solution, the DNA expands and is hydrated, yielding an average RI of ~1.38 for the surface of AuNP compared with 1.33 in water.

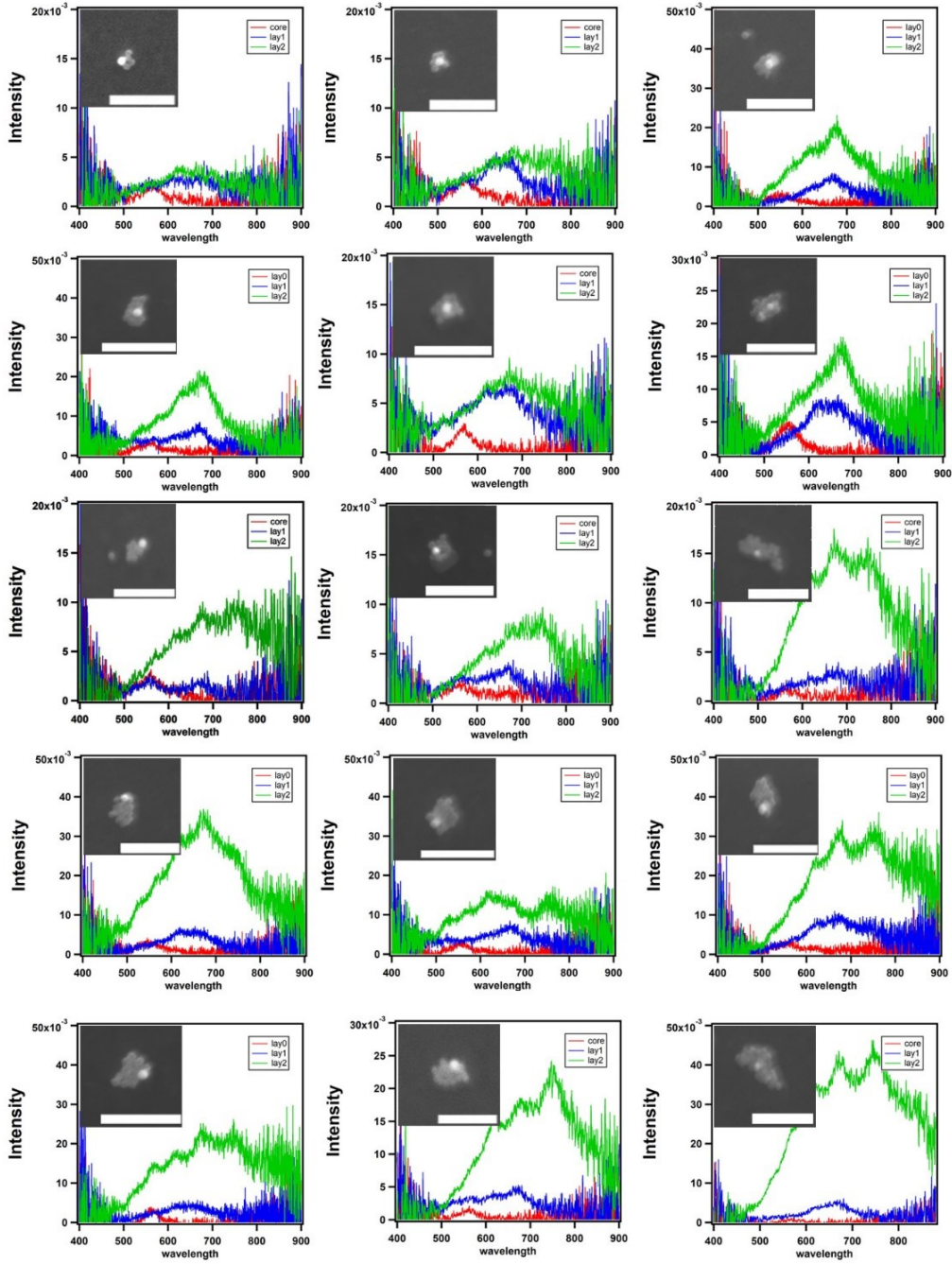


**Figure S4.** Correlated scanning electron microscopy (SEM) and single-nanostructure spectroscopy characterization of solid-shell assemblies. Scattering spectra of a single assembly with an increasing number of layers of satellite nanoparticles: red, 0-satellite layer; blue, 1-satellite layer; and green, 2-satellite layers. Inset shows SEM image after 2 layers of assembling. Scale bar: 500 nm.

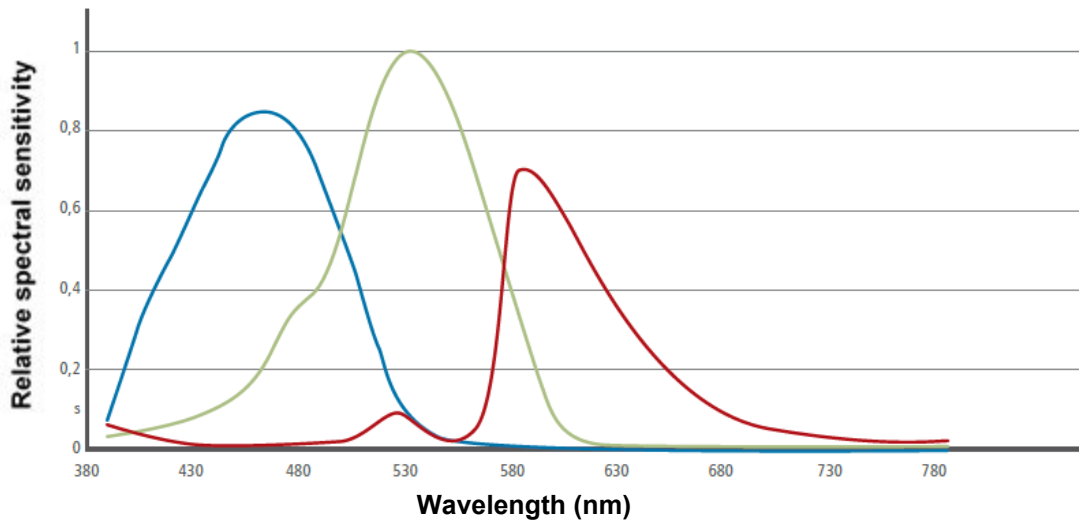


**Figure S5.** Measured relative spectral sensitivity of the color CCD camera from the manufacturer.

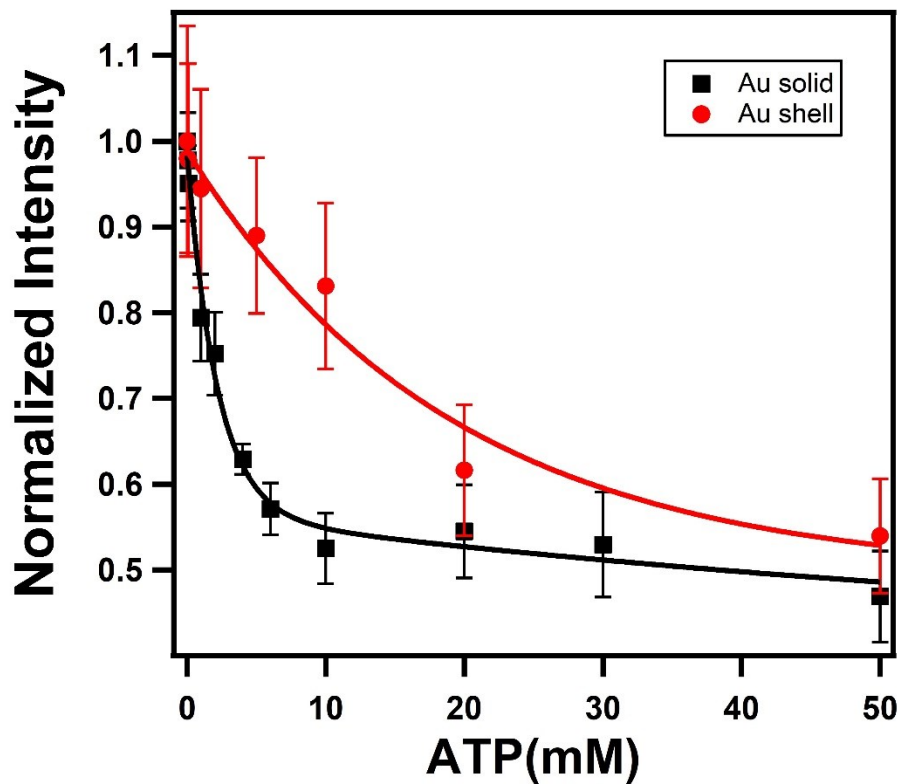


**Figure S6.** Comparison of calibration curves for solid-solid (black) vs solid-shell (red curve) assemblies. The fitted parameters of the two calibration curves (shown in Table S2) are significantly different at 95 % confidence level based on the F-test and Chow test.<sup>2</sup>

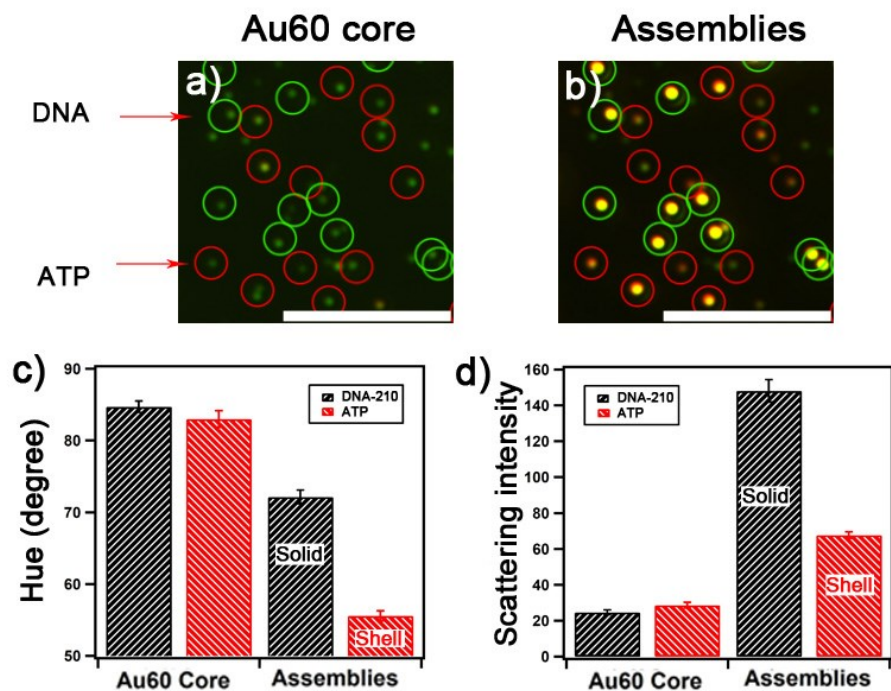


**Figure S7.** Optical properties of duplexed sensors comprising DNA-210 (solid-solid) and ATP-targeting (solid-shell) assemblies. Darkfield images of (a) 60-nm core AuNP functionalized with two sequences of DNA (green for DNA-210 and red for ATP), and (b) after assembly with the satellite particles (solid and shell, respectively). Average (c) hue and (d) scattering intensity of assemblies obtained from darkfield images. Error bars are standard deviations of independent experiments. Scale bar: 10  $\mu\text{m}$ .



## SUPPORTING TABLES

**Table S1.** Loading of DNA on 30-nm solid AuNP and 45-nm Au nanoshells.

| <b>Sample</b>   | <b>Concentration of particle (nM)</b> | <b>Concentration of DNA (<math>\mu\text{M}</math>)</b> | <b>Number of strands per particle</b> |
|-----------------|---------------------------------------|--|---------------------------------------|
| Au30_Seq 1      | 0.66                                  | 0.15   | 234 $\pm$ 12                          |
| Au30_Seq 2      | 0.66                                  | 0.27   | 410 $\pm$ 11                          |
| Aushell45_Seq 1 | 0.106                                 | 0.079  | 749 $\pm$ 25                          |
| Aushell45_Seq 2 | 0.106                                 | 0.10   | 961 $\pm$ 13                          |

**Table S2.** Fitted parameters of calibration curves in Fig. 4 to the equation  $y = y_0 + a \frac{K_{[]x}}{1+K_{[]x}}$ .

The detection limit was calculated based on the signal of  $y_0 - 3s$  where  $s$  is the standard deviation of the image intensity or hue between replicates of experiments.

|                             | Fitted parameters |            |             | Detection limit (mM) | s   |
|-----------------------------|-------------------|------------|-------------|----------------------|-----|
|                             | $K_{[]}$          | $y_0$      | a           |                      |     |
| Solid-solid assembly (int.) | 0.53± 0.09        | 98.2 ± 1.7 | -60.4 ± 2.3 | 0.23                 | 3.7 |
| Solid-shell assembly (int.) | 0.07 ± 0.01       | 67.6 ± 1.3 | -37.1 ± 2.0 | 3.2                  | 3.3 |
| Solid-shell assembly (Hue)  | 0.05 ± 0.01       | 47.3 ± 0.9 | 24.9 ± 1.6  | 3.7                  | 1.3 |

### Supporting Reference

- (1) Elhadj, S.; Singh, G.; Saraf, R. F. *Langmuir* **2004**, *20*, 5539–5543.
- (2) Chow, G. C. *Econometrica* **1960**, *28*, 591.